

# A Density Functional Theory Study of the Interaction between CO and O on a Pt Surface: CO/Pt(111), O/Pt(111), and CO/O/Pt(111)

K. Bleakley and P. Hu\*

Contribution from the School of Chemistry, The Queen's University of Belfast, Belfast BT9 5AG, UK

Received September 21, 1998. Revised Manuscript Received June 2, 1999

**Abstract:** Ab initio total energy calculations within the Density Functional Theory framework were carried out for Pt(111), Pt(111)-p(2×2)-CO, Pt(111)-p(2×2)-O, and Pt(111)-p(2×2)-(CO+O) to provide an insight into the interaction between CO and O on metal surfaces, an important issue in CO oxidation, and also in promotion and poisoning effects of catalysis. The geometrical structures of these systems were optimized with respect to the total energy, the results of which agree with existing experimental values very well. It is found that (i) the local structures of Pt(111)-p(2×2)-(CO+O), such as the bond lengths of C–O, C–Pt, and O–Pt (chemisorbed O atom with Pt), are almost the same as that in Pt(111)-p(2×2)-CO and Pt(111)-p(2×2)-O, respectively, (ii) the total valence charge density distributions in Pt(111)-p(2×2)-(CO+O) are very similar to that in Pt(111)-p(2×2)-CO, except in the region of the chemisorbed oxygen atom, and also nearly identical to that in Pt(111)-p(2×2)-O, apart from in the region of the chemisorbed CO, and (iii) the chemisorption energy of CO on a precovered Pt(111)-p(2×2)-O and the chemisorption energy of O on a precovered Pt(111)-p(2×2)-CO are almost equal to that in Pt(111)-p(2×2)-CO and Pt(111)-p(2×2)-O, respectively. These results indicate that the interaction between CO and chemisorbed oxygen on a metal surface is mainly short range in nature. The discussions of Pt–CO and Pt–O bonding and the interaction between CO and the chemisorbed oxygen atom on Pt(111) are augmented by local densities of states and real space distributions of quantum states.

## 1. Introduction

It is well-known that heterogeneous catalysis in which reactions often occur on solid surfaces is a very important subject in chemistry. Two major mechanisms have been proposed for catalytic reactions of two reactants on solid surfaces, namely Eley–Rideal and Langmuir–Hinshelwood. In the Eley–Rideal mechanism, one reactant adsorbs on a solid surface first, and then another species reacts with the chemisorbed reactant directly from the gas phase, forming a product. In the Langmuir–Hinshelwood mechanism, on the other hand, there are three steps: (i) both reactants adsorb on a solid surface; (ii) they diffuse toward each other or one to the other along the surface and react to form a product; and (iii) the product desorbs from the surface. Most catalytic reactions follow the Langmuir–Hinshelwood mechanism while only a few have been found to obey the Eley–Rideal mechanism.<sup>1,2</sup> Obviously, a sound understanding of the Langmuir–Hinshelwood mechanism is crucial for insight into heterogeneous catalysis. The first step and the third step in the Langmuir–Hinshelwood mechanism have been extensively studied in the last three decades, and a great deal of knowledge has been accumulated.<sup>3,4</sup> However, little is known about the second step which is generally the most important one among the three steps. To provide insight into

the second step, an understanding of how two chemisorbed species interact on solid surfaces is of importance. In this paper we report a theoretical study on Pt(111), CO/Pt(111), O/Pt(111), and CO/O/Pt(111), using Density Functional Theory, aiming to shed some light on this issue.

In fact, the interaction between chemisorbed species on solid surfaces, particularly metal surfaces, has long been a hot subject. On the basis of the effective-medium theory, Norskov, Holloway, and Lang<sup>5</sup> suggested that the interaction between both electronegative (e.g. O, S, Cl) and electropositive (e.g. Na, K) species and molecules (e.g. CO, H<sub>2</sub>) is mainly electrostatic in nature. Feibelman and Hamann<sup>6</sup> calculated the local density of states at the Fermi level for S/Rh(001) using a self-consistent linearized-augmented-plane-wave method and concluded that the interaction between S and molecules is long range in nature. Luftman, Sun, and White<sup>7</sup> carried out extensive studies on coadsorption of CO and K on Ni(100). In interpreting their experimental results, a long-range interaction between adsorbates was favored. Dorsett and Reutt–Robey<sup>8</sup> monitored CO–O coadsorption-induced changes on Ni(119) using infrared reflection–absorption spectroscopy and found that virtually all the CO on the terraces shifts from atop to bridge sites when O fully saturates sites of the step edge. They suggested that the through-metal CO–O interaction must be operative over a range of 5 Å. On the other hand, using angle-resolved photoemission spectra from coadsorption of CO and K on Cu(100) and Ru(0001), Eberhardt et al.<sup>9</sup> found that there is a large shift of the

\* Corresponding author. Fax: (+44) 1232 382177. E-mail: p.hu@qub.ac.uk.

(1) Kuipers, E. W.; Vardi, A.; Danon, A.; Amirav, A. *Phys. Rev. Lett.* **1991**, *66*, 116.

(2) Rettner, C. T. *Phys. Rev. Lett.* **1992**, *69*, 383.

(3) Somojar, G. A. *Introduction to Surface Chemistry and Catalysis*; John Wiley and Sons: New York, 1994. Ertl, G.; Kuppers, J. *Low Energy Electrons and Surface Chemistry*; VCH Verlagsgesellschaft: Weinheim, 1985.

(4) Hoffmann, R. *Rev. Mod. Phys.* **1988**, *60*, 601. Hoffmann, R. *Solids and Surfaces: A Chemists View of Bonding in Extended Structures*; VCH: New York, 1988.

(5) Norskov, J. K.; Holloway, S.; Lang, N. D. *Surf. Sci.* **1984**, *137*, 65.

(6) Feibelman, P. J.; Hamann, D. R. *Phys. Rev. Lett.* **1984**, *52*, 61.

(7) Luftman, H. S.; Sun, Y. M.; White, J. M. *Surf. Sci.* **1984**, *141*, 82.

(8) Dorsett, H. E.; Reatt–Robey, J. E. *Surf. Sci.* **1997**, *380*, 165.

(9) Eberhardt, W.; Hoffmann, F. M.; De Pola, R.; Heskett, D.; Strathy, I.; Plummer, E. W.; Moser, H. R. *Phys. Rev. Lett.* **1985**, *54*, 1856.

$1\pi$  molecular orbital of CO. They suggested that the interaction between CO and K is short range. The same conclusion was obtained by Woodruff and co-workers.<sup>10</sup> It is clear that further studies concerning these long- and short-range interactions are required.

CO and oxygen chemisorption on Pt(111) was chosen in this study. The motivation for this was 2-fold. First, CO oxidation is one of the most important catalytic reactions. Technologically it is one of the major reactions occurring in car exhaust catalytic converters, which have been widely used since the 1970s to remove CO and other pollutants. It is also important in several other technologies such as CO<sub>2</sub> lasers, air purification, and sensors. Scientifically, CO oxidation is one of the simplest catalytic reactions, which can be considered as an ideal model system to tackle. Therefore, it is not surprising that CO oxidation has been a hot subject in the last 30 years. Despite its simplicity and the large volume of work carried out in this field, many fundamental questions remain unanswered. Second, promotion and poisoning effects are very important issues in catalysis. These can be achieved by adding a species, such as Na, K, and S, which can significantly affect the reactivity of catalysts. It is known that the electronegativity of oxygen is very high, and it is expected to play an important role in coadsorbate systems. Therefore, the CO + O coadsorbate system can be considered as a model to study promotion and poisoning effects in catalysis.

In this paper, we intend to answer the following questions: (i) What is the stable structure of Pt(111)-(2×2)-(CO+O) before CO oxidation? (ii) Is the interaction between chemisorbed CO and chemisorbed oxygen on Pt(111) long or short range in nature? (iii) Why is this interaction short or long range? Obviously, an answer to the first question is the first step in tackling the second and third questions.

This paper is organized as follows. The methodology of our theoretical approach is outlined in the second section. The results of the clean Pt(111) surface are presented in the first part of section 3. The second and third parts of section 3 contain results of CO/Pt(111) and O/Pt(111). The results of CO + O coadsorption on Pt(111) are shown in the last part of section 3. Conclusions are summarized in the final section.

## 2. Calculations

Ab initio total energy calculations were carried out using Density Functional Theory. The electronic ground states of systems are directly obtained by a kind of Car–Parrinello approach,<sup>11</sup> the conjugate gradients minimization,<sup>12</sup> instead of conventional matrix diagonalization. Wave functions are expanded in plane waves. A Fermi surface smearing of 0.1 eV was used to speed up the convergence of  $\mathbf{k}$ -sampling and the energy extrapolated to zero temperature using the method of Gillan and De Vita.<sup>13,14</sup> Ab initio pseudopotentials in fully separable Kleinman–Bylander form were generated by a kinetic energy filter optimization scheme in which electrons of 2s and 2p in C, 2s and 2p in O, and 5d, 6s, and 6p in Pt were treated as valence electrons and the rest of the electrons were included in core potentials.<sup>15</sup>

Recent studies<sup>16–18</sup> have shown that geometrical structures of molecules and solids determined by local density approximation (LDA)

(10) Somerton, C.; McConville, C. S.; Woodruff, D. P.; Grider, D. E.; Richardson, N. V. *Surf. Sci.* **1984**, *138*, 31.

(11) Car, R.; Parrinello, M. *Phys. Rev. Lett.* **1985**, *55*, 55.

(12) Payne, M. C.; Teter, M. P.; Allen, D. C.; Arias, T. A.; Joannopoulos, J. D. *Rev. Mod. Phys.* **1992**, *64*, 1045.

(13) Gillan, M. J. *J. Phys.: Condens. Matter* **1989**, *1*, 689.

(14) De Vita, A.; Gillan, M. J. *J. Phys.: Condens. Matter* **1995**, *3*, 1731.

(15) Lin, J.-S.; Qteish, A.; Payne, M. C.; Heine, V. *Phys. Rev. B* **1993**, *47*, 4174.

(16) Hu, P.; King, D. A.; Crampin, S.; Lee, M.-H.; Payne, M. C. *Chem. Phys. Lett.* **1994**, *230*, 501.

(17) Hu, P.; King, D. A.; Lee, M.-H.; Payne, M. C. *Chem. Phys. Lett.* **1995**, *246*, 73.

calculations are very reasonable compared to experimental work and that no considerable improvement is obtained with gradient corrections. On the other hand, chemisorption energies obtained with LDA are significantly higher than experimental values, while calculation results with gradient corrections agree with experimental data very well. It was also found that sites for adsorption with higher coordination of the adsorbate to surface atoms lead to a larger degree of overbinding with LDA, and give larger corrections with gradient corrections.<sup>16</sup> In this study, all structure optimizations were carried out with LDA, in which the Ceperly–Alder exchange-correction energy was used; the generalized gradient approximation (GGA) of Perdew and Wang<sup>19</sup> was utilized in gradient correction calculations.

Some physical and chemical properties of CO, bulk Pt, and some chemisorption systems were tested. Agreement with experimental work, such as CO bond length (error 0.02%), CO vibrational frequency (error 1%), and Pt lattice constant (error 0.3%), is very reasonable.

## 3. Results and Discussions

**3.1. Clean Pt(111).** The structure of the clean Pt(111) was calculated using a 4-layer Pt slab by fixing the bottom 3 layers at their bulk positions according to the calculated lattice constant (3.93 Å, experimental value 3.92 Å) and allowing the top layer to relax. It was found that the surface layer relaxation is negligible, i.e., the top layer of the surface remains in its bulk-truncated position.

Some years ago, Adams et al.<sup>20</sup> measured and analyzed Low Energy Electron Diffraction intensity–voltage spectra (LEED  $I$ – $V$ ) from clean Pt(111). They found that there is a 1% expansion of the first layer spacing. Later, Hayek et al.<sup>21</sup> used the same technique to study the same system and concluded that there is no surface relaxation. This result was confirmed by Ogletree et al.<sup>22</sup> A recent study<sup>23</sup> reported a 1% expansion of the first layer spacing. Our calculated geometrical structure agrees very well with these experimental results.

**3.2. CO/P(111).** CO chemisorption on metal surfaces has been substantially studied both experimentally and theoretically.<sup>24–27</sup> At low temperatures, adsorption of CO on Pt(111) at low coverage gives rise to a LEED pattern corresponding to (4×4) and (8×8) structures.<sup>28</sup> A single band of infrared spectra at 2089 cm<sup>-1</sup> was observed, which was assigned to CO on the top site. Longer CO exposures give rise to a sharp c(4×2) pattern that corresponds to CO coverage of 0.5 ML (ML = monolayer). Infrared spectra reveal two bands, one being assigned to CO chemisorption on the top sites and the other on the bridge sites. Ogletree et al.<sup>22</sup> performed detailed LEED  $I$ – $V$  analysis on Pt(111)-c(4×2)-CO and found that there are two types of CO molecules in a unit cell, one adsorbing on the bridge site with a C–O bond length of 1.15 Å and a C–Pt bond length of 2.08 Å and the other on the top site with a C–O bond length of 1.15 Å and a C–Pt bond length of 1.85 Å. The chemisorption energies of CO on Pt(111) were experimentally measured by

(18) Hu, P.; King, D. A.; Crampin, S.; Lee, M.-H.; Payne, M. C. *J. Chem. Phys.* **1997**, *107*, 8103.

(19) Perdew, J. P. In *Electronic Structure of Solids*; Ziesche, P., Eschrig, H., Eds.; Akademie Verlag: Berlin, 1991.

(20) Adams, D. L.; Nielsen, H. B.; Van Hove, M. A. *Phys. Rev. B* **1979**, *20*, 4789.

(21) Hayek, K.; Glassl, H.; Gutman, A.; Leonhard, H.; Prutton, M.; Tear, S. P.; Weltoncook, M. R. *Surf. Sci.* **1985**, *152/153*, 419.

(22) Ogletree, D. F.; Van Hove, M. A.; Somorjai, G. A. *Surf. Sci.* **1986**, *173*, 351.

(23) Materer, N.; Starke, U.; Barbieri, A.; Doll, R.; Heinz, K.; Van Hove, M. A.; Somorjai, G. A. *Surf. Sci.* **1995**, *325*, 207.

(24) Blyholder, G. *J. Phys. Chem.* **1964**, *68*, 2772.

(25) Blyholder, G.; Allen, M. C. *J. Am. Chem. Soc.* **1969**, *91*, 3158.

(26) Wong, Y.-T.; Hoffmann, R. *J. Phys. Chem.* **1991**, *95*, 859.

(27) Mehandru, S. P.; Anderson, A. B. *Surf. Sci.* **1988**, *201*, 345.

(28) Tushaus, M.; Schweizer, E.; Hollins, P.; Bradshaw, A. M. *J. Electron Spectrosc.* **1987**, *44*, 305.

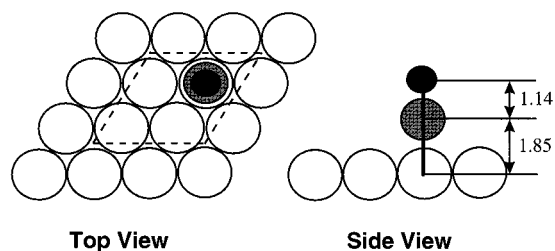


**Figure 1.** Schematic illustration of geometry of CO chemisorption on the atop site of Pt(111). The  $p(2 \times 2)$  unit cell is indicated in dashed lines.

**Table 1.** A Comparison of Our Calculated C–O and C–Pt Bond Lengths for CO/Pt(111) with Experimental Results<sup>22</sup>

	C–O bond length (Å)	C–Pt bond length (Å)
calculated	1.14	1.85
experimental <sup>22</sup>	1.15	1.85

Yeo et al.<sup>29</sup> using the calorimetric method. It was reported that the chemisorption energies decrease from around 1.9 eV at low coverages to 1.2 eV at half monolayer coverage.<sup>29</sup>

In this study, CO chemisorption on Pt(111) was modeled using a  $p(2 \times 2)$  unit cell with CO on the top site, which is schematically shown in Figure 1. A  $p(2 \times 2)$  unit cell was chosen for two reasons. First, one of the goals in this study is to determine the binding strength between CO and Pt(111) with the minimum interaction between CO molecules. Certainly, the lower the CO coverage is, the less the interaction between CO molecules will be, but this requires greater computational cost. A  $p(2 \times 2)$  unit cell seems to be a good compromise. Second, we intend to directly compare CO/Pt(111) with Pt(111)- $p(2 \times 2)$ -O and Pt(111)- $p(2 \times 2)$ -(CO+O), which are well characterized experimentally.<sup>23,30</sup> In our calculations, the Pt(111) substrate was modeled by 3 layers of Pt, being fixed at the positions as the clean surface structure, while C and O atoms were allowed to move in all directions to lower the energies according to the forces calculated using the Hellmann–Feynman theorem. The final optimized structure parameters are listed in Table 1. It is clear that there is good agreement between our calculated structure and experimental values. The chemisorption energy of CO was found to be 1.55 eV, obtained by subtracting the total energy of CO/Pt(111) from the total energies of the CO molecule and the Pt substrate, which is in reasonable agreement with experiment.<sup>29</sup>

To understand CO chemisorption and to further shed light upon the interaction between CO and O, we calculated a local density of states around CO from Pt(111)- $p(2 \times 2)$ -CO. In the calculations of the local density of states, a cylinder around CO with a radius of 0.4 Å was used. The local density of states is displayed in Figure 2a. To show a comparison, we also calculated a local density of states from a CO molecule, displayed in Figure 2b. It can be seen that the first peak in Figure 2a appears at almost the same energy level as the CO  $3\sigma$  peak. By examining the quantum states in CO/Pt(111), we found that the states within this peak contain strong  $3\sigma$  character. A typical quantum state in this peak is shown in Figure 3b. It is clear that it is almost identical to the original CO  $3\sigma$  orbital, shown in Figure 3a. The second peak of Figure 2a centered at  $-15$  eV contains strong CO  $4\sigma$  orbital character, which can be seen in a quantum state plot in Figure 3d. The CO  $4\sigma$  orbital is shown in Figure 3c. On the other hand, d character is apparent in the

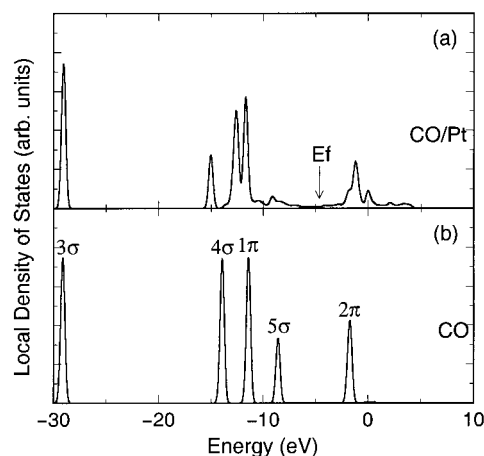


**Figure 2.** Local densities of states calculated by cutting a cylinder with a radius of 0.4 Å around CO from CO/Pt(111) (a) and CO (b). The Fermi level is indicated by the arrow.

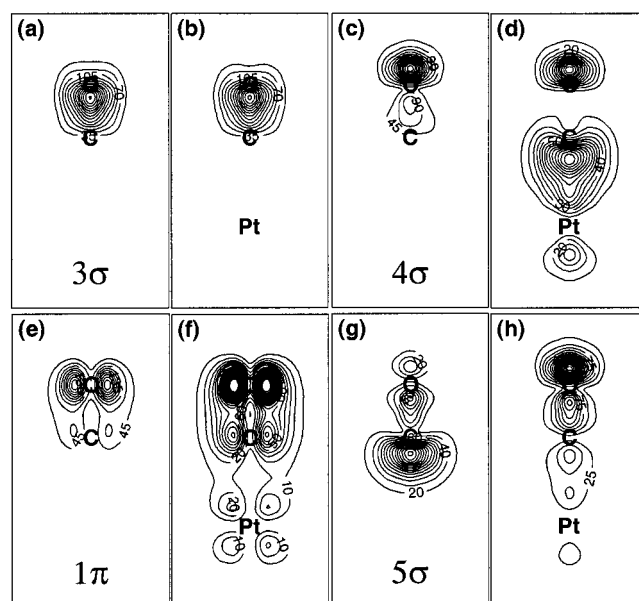


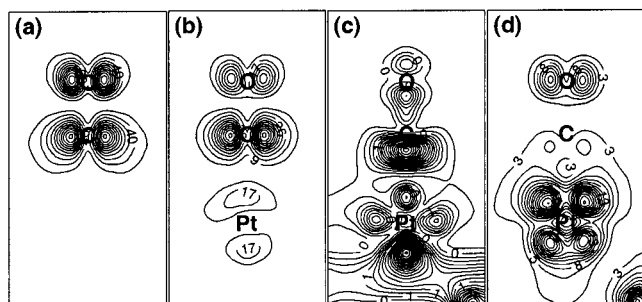
**Figure 3.** Charge density comparisons between the  $3\sigma$ ,  $4\sigma$ ,  $1\pi$ , and  $5\sigma$  orbitals of the CO molecule and  $3\sigma$ -,  $4\sigma$ -,  $1\pi$ -, and  $5\sigma$ -derived orbitals from Pt(111)- $p(2 \times 2)$ -CO. Panels a, c, e, and g are 2D contours of charge densities of the CO  $3\sigma$ ,  $4\sigma$ ,  $1\pi$ , and  $5\sigma$  orbitals respectively, cutting through the C–O bond axes. Panels b, d, f, and h are 2D contours of charge densities of  $3\sigma$ -,  $4\sigma$ -,  $1\pi$ - and  $5\sigma$ -derived orbitals from Pt(111)- $p(2 \times 2)$ -CO, which correspond to states,  $\psi_{\mathbf{k}}(E)$ , at  $\mathbf{k} = (0.125, 0.125, 0.0)$ ,  $E = -24.43, -10.50, -7.14, \text{ and } -8.00$  eV, respectively, where the Fermi level is defined as zero. A linear scale is used in units of  $10^{-3}$  electrons/bohr<sup>3</sup>.

quantum states within the peak and also the peak position shifts considerably downward compared to that of the original CO  $4\sigma$  peak. Since there is a charge accumulation between the C and a metal atom in these types of states, they can be considered as kinds of bonding states. The quantum states in the third peak of Figure 2a consists of strong  $5\sigma$  and quite strong metal d character. A typical quantum state in the third peak is shown in Figure 3h. The striking feature in this quantum state is that there is a strong charge accumulation between the C and the metal atom, indicating its important role in holding CO on the surface. The energy levels of these states are substantially lower than the CO  $5\sigma$  orbital due to the strong mixing, which is in agreement with previous work.<sup>31,32</sup>  $1\pi$  derived states, which contain strong  $1\pi$  character and weak d character, shown in

(29) Yeo, Y. Y.; Vattuone, L.; King, D. A. *J. Chem. Phys.* **1997**, *106*, 392.

(30) Yoshinobu, J.; Kawai, M. *J. Chem. Phys.* **1995**, *103*, 3220.





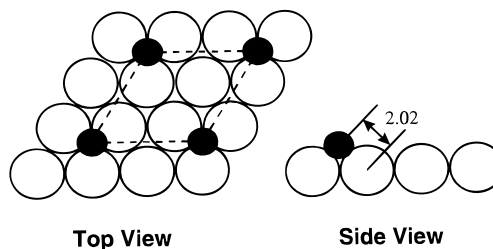
**Figure 4.** Illustration of quantum states with  $5\sigma$  and  $2\pi$  character in the metal band region and above the Fermi level. Panel a shows 2D contours of charge densities of the  $2\pi$  orbital from a CO molecule. Panel b shows 2D contours of charge densities of a quantum state above the Fermi level. Panels c and d show two quantum states in the metal band region, which contain  $5\sigma$  and  $2\pi$  character, respectively. Note that there is a slight charge accumulation between CO  $5\sigma$  and the side of Pt d in panel c, and the charge density distribution around the CO in panel d is quite different from the CO  $2\pi$  orbital. A linear scale is used in units of  $10^{-3}$  electrons/bohr<sup>3</sup>.

Figure 3f can be found to be in the fourth peak. In the fifth peak in Figure 2a strong  $2\pi$  character can be seen. A typical quantum state in this peak is shown in Figure 4b, in which there is a nodal surface between the C and the metal atom.

In the region between the fourth peak and the Fermi energy in Figure 2a, in which the original metal states locate, some  $5\sigma$  and also  $2\pi$  character of CO can be found. Typical quantum states with  $5\sigma$  and  $2\pi$  character in this region are shown in Figure 4, panels c and d, respectively. Although molecular character is quite weak in this region, it plays a very important role in chemisorption systems. In particular, the existence of the quantum states shown in Figure 4d is of importance in CO chemisorption systems. First, they are mainly responsible for weakening the CO bond; and second, a large portion of the chemisorption energy can be attributed to these states.<sup>33</sup>

**3.3. O/Pt(111).** The chemisorption of oxygen atoms on Pt surfaces has been extensively studied by a range of experimental techniques. Pt(100) is a complex system: there are two different structures and they exhibit distinguished chemical reactivities. One is the unreconstructed ( $1\times 1$ ) phase which is 0.21 eV less stable than the other which is a reconstructed quasihexagonal structure.<sup>34</sup> Norton et al.<sup>35</sup> found that at 123 K, O<sub>2</sub> adsorbs dissociatively on the ( $1\times 1$ ) surface while dissociation does not occur on the reconstructed hex surface. In contrast, Pt(111) is a rather simple system: there is no lateral reconstruction and surface layer relaxation is extremely small (1% expansion reported in refs 20 and 23, 0% expansion reported in refs 21 and 22). It is known that oxygen molecules dissociate on Pt(111) with small barriers.<sup>36</sup> Materer et al.<sup>23</sup> carried out LEED  $I-V$  analysis for Pt(111)-p( $2\times 2$ )-O and found that oxygen atoms adsorb on fcc hollow sites with an O–Pt bond length of 2.02 Å.

In this study, oxygen atom chemisorption was modeled using a p( $2\times 2$ ) unit cell corresponding to an oxygen coverage of 0.25 ML. Oxygen atoms were placed on fcc hollow sites, shown in Figure 5. The bond length of O–Pt was optimized according



**Figure 5.** Schematic illustration of the geometry of O chemisorption on a 3-fold hollow site of Pt(111). The p( $2\times 2$ ) unit cell is indicated in dashed lines.

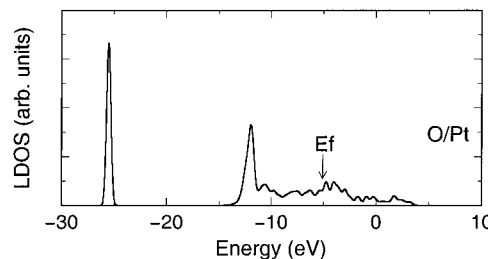


**Figure 6.** A local density of states calculated by cutting a sphere with a radius of 0.4 Å around the O atom from Pt(111)-p( $2\times 2$ )-O. The Fermi level is indicated by the arrow.

to forces calculated using the Hellmann–Feynman theorem. It was found that the calculated bond length of O–Pt is 2.02 Å, which agrees with experimental data (2.02 Å)<sup>23</sup> very well. The chemisorption energy was found to be 4.43 eV, which is in reasonable agreement with the results of a previous study.<sup>37</sup> Compared to CO chemisorption, the bonding between oxygen atoms and metal surfaces is less well understood. An earlier theoretical work of oxygen atom chemisorption on Pt(100) was carried out by Bullett and Cohen.<sup>38</sup> Using a localized orbital method, they performed calculations for a c( $2\times 2$ ) oxygen overlayer on Pt(100). Local densities of states from the system were presented and it was concluded that oxygen atoms should adsorb on the 4-fold hollow sites. However, a recent DFT study by Ge et al.<sup>39</sup> contradicts this conclusion. It was found that the most stable adsorption site for a c( $2\times 2$ ) oxygen overlayer on Pt(100)-( $1\times 1$ ) is the bridge site. It was reported<sup>39</sup> that no metal character mixing with the oxygen 2s orbital is observed while mixing between oxygen p orbitals and the d-bands of Pt spreads throughout the Pt d-band energy range.

To further understand the bonding between O and Pt surfaces, we calculated a local density of states by cutting a sphere with a 0.4 Å radius around the O atom in O/Pt(111). The local density of states is shown in Figure 6. We found that the quantum states in O/Pt(111) within the first peak in Figure 6 are similar to the 2s orbital of an isolated oxygen atom, shown in Figure 7. However, by closely examining the quantum states, some differences can be observed. First, a considerable distortion from the spherical distribution in the quantum state can be seen. Second, the center of the electron densities moves slightly toward the surface. Third, the energy levels of the quantum state from O/P(111) are lower than the s orbital of an isolated oxygen atom. The electron density redistribution can be clearly seen in Figure 7c, in which the same cut of electron density difference between the quantum state from O/P(111) shown in Figure 7b

(31) Wimmer, E.; Fu, C. L.; Freeman, A. *J. Phys. Rev. Lett.* **1985**, *55*, 2618.

(32) Chen, R.; Satoko, C. *Surf. Sci.* **1989**, *223*, 101.

(33) Hammer, B.; Morikawa, Y.; Norskov, J. K. *Phys. Rev. Lett.* **1996**, *76*, 2141.

(34) Yeo, Y. Y.; Wartnaby, C. E.; King, D. A. *Science* **1995**, *268*, 1731.

(35) Norton, P. R.; Binder, P. E.; Griffiths, K. J. *Vac. Sci. Technol.* **1984**, *A2*, 1028.

(36) Eichler, A.; Hafner, J. *Phys. Rev. Lett.* **1997**, *79*, 4481.

(37) Hammer, B.; Norskov, J. K. In *Chemisorption and Reactivity on Supported Clusters and Thin Films*; Lambert, R. M., Pacchioni, G., Eds.; Kluwer Academic Publishers, The Netherlands, 1997; p 285.

(38) Bullett, D. W.; Cohen, M. L. *J. Phys. C: Solid State Phys.* **1977**, *10*, 2101.

(39) Ge, Q.; Hu, P.; King, D. A.; Lee, M.-H.; White, J. A.; Payne, M. C. *J. Chem. Phys.* **1997**, *106*, 1210.

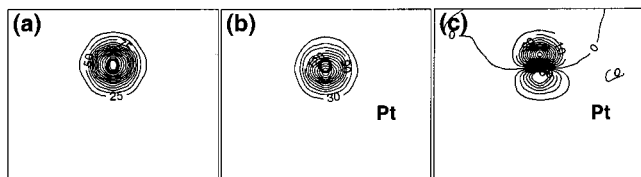


**Figure 7.** Illustration of the polarization of the O 2s orbital in O/Pt(111). Panels a and b are 2D contours of charge densities of the 2s orbital from an isolated O atom and the lowest energy valence electron orbital from O/Pt(111), respectively. Panel c is the 2D contours of the difference between panel b and panel a, (b - a). The top region is negative and the bottom region is positive.

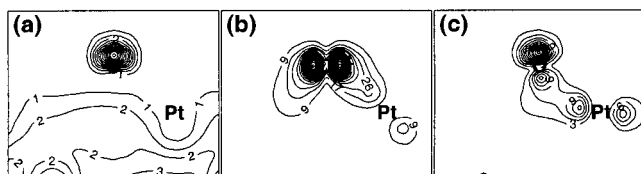


**Figure 8.** Illustration of the bonding between O p orbitals and metal states. Panels a-c show 2D contours of charge densities of quantum states,  $\psi_{\mathbf{k}}(E)$ , at  $\mathbf{k} = (0.125, 0.125, 0.0)$ ,  $E = -9.16, -7.26,$  and  $-7.10$  eV, respectively, where the Fermi level is defined as zero. A linear scale is used in units of  $10^{-3}$  electrons/bohr<sup>3</sup>.

and the s orbital from an isolated O atom displayed in Figure 7a is illustrated. It is obvious that there is a charge polarization toward the metal, although the mixing between metal states and the oxygen s orbital is not significant.

The second band in the O/Pt(111) system mainly contains states which have O  $p_z$  character with the bottom lobe of  $p_z$  delocalized almost completely into the metal. Because of this delocalization, the kinetic energies of these states are much lower than other states in the O/Pt(111) system. A typical quantum state of this kind is shown in Figure 8a. It should be noted that the energy levels of these states are about -13.5 eV and they do not have a great weight in the local density of states due to their delocalized nature.

A typical quantum state within the second peak in Figure 6 is shown in Figure 8b. It is a mixing state between a strong oxygen p orbital and a relatively weaker metal d state. The energy level of this quantum state is several eV lower than the p orbital of an isolated oxygen atom, due to the strong mixing. Above the second peak up to the Fermi level, as Figure 6 shows, there is quite an even distribution of the local density of states around the oxygen atom in O/Pt(111). By examining all the quantum states in our calculations in this region, we found that they are mixing states between quite strong oxygen p and very strong metal d orbitals. A typical state is shown in Figure 8c.

On the basis of the above analysis, we propose the following interaction diagram, shown in Figure 9. The energy levels of atomic orbitals are displayed on the right-hand side, the metal bands are shown on the left-hand side, and the energy bands of O/Pt(111) are illustrated in the middle. The mixing between the oxygen s orbital and metal states is extremely small, while the polarization in these states is significant. Because of the localized nature of these states on the oxygen atom, they form a very narrow band at low oxygen coverages. Next, the oxygen p orbitals mix strongly with metal states to form a few energy bands, in which the oxygen p character is slightly stronger than the metal character. Then in the region corresponding to metal-derived states, metal d states mix strongly with the oxygen p orbitals.

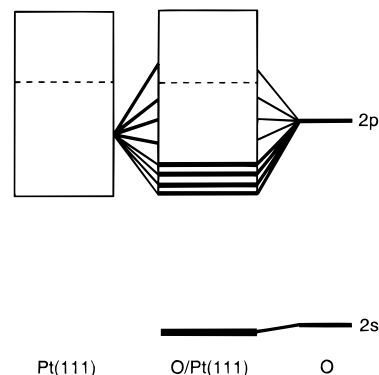


**Figure 9.** Schematic illustration of the interaction between O atomic orbitals and a Pt surface.

**3.4. CO/O/Pt(111).** Coadsorbate systems, such as CO + K<sup>40</sup> and CO + O,<sup>41-43</sup> have received more interest recently partially due to the desire for an understanding of promotion and poisoning effects in catalysis and partially because recent advances in surface science technologies have made careful studies of such complex systems possible. In particular, coadsorbate systems of CO + O are very interesting for several reasons. First, they are the initial step in CO oxidation and an understanding of such systems is crucial in providing insight into the CO oxidation. For example, the answers to questions, such as what are the structural differences between CO/O/metal and CO or oxygen on the same metal surface, and what are the bonding differences in these systems, are necessary in order to understand CO oxidation. Second, because of high electronegativity of the oxygen atom, the coadsorbate systems of CO + O can be used as model systems to study promotion and poisoning effects in catalysis.

The structures of only a few CO + O systems have been quantitatively determined. This is because first, the unit cells of such systems are usually quite large and therefore a full structure search is very time-consuming. Second, ordered phases in such systems are rare and relatively difficult to prepare experimentally. Narloch, Held, and Mensel<sup>42</sup> prepared a Ru(001)-p(2×2)-(CO+O) by precovering the clean surface with a p(2×2) oxygen layer and subsequently dosing CO at low temperatures. They measured LEED  $I-V$  spectra from the system and searched for the geometrical structure using Tensor LEED. It was found that the C-O bond length, 1.16 Å, in the (CO + O) coadsorbate system is almost the same as that of Ru(001)-( $\sqrt{3} \times \sqrt{3}$ )R30°-CO (1.17 Å),<sup>44</sup> while the C-metal distance in the coadsorbate system is 1.93 Å, decreasing slightly compared to 1.98 Å, the C-metal distance in the pure CO on Ru(001). The bond lengths between adsorbed O atoms and nearest neighbor metal atoms are 2.06 and 2.09 Å, respectively (two different nearest neighbors). These are slightly longer than that in O/Ru(001) (2.03 Å).<sup>45</sup> By exposing a precovered Rh(111)-p(2×2)-O surface to 20 L of CO at a temperature of 200 K and subsequently heating to 370 K, Schwegmann, Over, De Renzi, and Ertl<sup>43</sup> obtained an ordered Rh(111)-p(2×2)-(CO+O). A quantitative LEED  $I-V$  analysis on the coadsorbate system shows that the bond lengths of C-O and C-Rh are 1.19 and

(40) Kaukasoina, P.; Lindroos, M.; Hu, P.; King, D. A.; Barnes, C. J. *Phys. Rev. B* **1995**, *51*, 17063.

(41) Narloch, B.; Held, G.; Menzel, D. *Surf. Sci.* **1994**, *317*, 131.

(42) Narloch, B.; Held, G.; Menzel, D. *Surf. Sci.* **1995**, *340*, 159.

(43) Schwegmann, S.; Over, H.; De Renzi, V.; Ertl, G. *Surf. Sci.* **1997**, *375*, 91.

(44) Over, H.; Moritz, W.; Ertl, G. *Phys. Rev. Lett.* **1993**, *70*, 315.

(45) Lindroos, M.; Held, G.; Pfor, H.; Menzel, D. *Surf. Sci.* **1989**, *222*, 451.

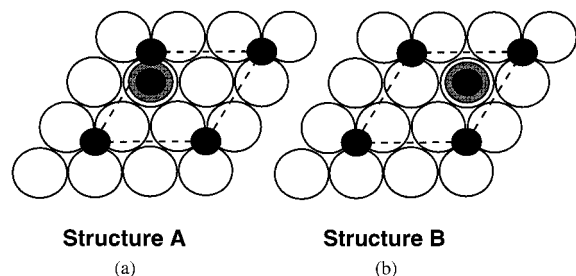


**Figure 10.** Schematic illustration of two different structures for Pt(111)-p(2×2)-(CO+O). Structure A was proposed in ref 30. We found that structure B is more stable than structure A.

1.83 Å, respectively, which is almost identical with that in pure CO chemisorption on the same surface (1.20 and 1.83 Å, respectively),<sup>46</sup> while the O–Rh bond length changes from 2.00 to 2.06 Å from pure oxygen chemisorption on Rh(111) to (CO + O) coadsorption.<sup>43</sup>

Despite the importance of Pt in CO oxidation, a quantitative structural determination of a (CO + O) coadsorbate system has not been reported yet. However, some structural information has been obtained experimentally. By dosing CO on a Pt(111)-p(2×2)-O, Yoshinobu and Kawai<sup>30</sup> obtained an ordered Pt(111)-p(2×2)-(CO+O) phase. A single sharp absorption peak at 2115 cm<sup>-1</sup> in the IRAS spectrum was observed, which was assigned to the C–O stretching frequency for CO on the top site. On the basis of the IRAS data and the fact that oxygen atoms adsorb on the fcc hollow sites, a model shown in Figure 10a was proposed.<sup>30</sup> A similar structure was also suggested for CO/O/Ni(111).<sup>47</sup>

In fact, the IRAS data suggest that CO is on the top site. However, there are actually two types of top sites, and therefore two different structures, one being shown in Figure 10a and other in Figure 10b. We calculated both structures. It was found that (i) structure A is not stable (CO and oxygen will move away from the top and hollow sites respectively if the structure is optimized) and (ii) structure B is much more stable (over 1 eV) than structure A if structure A is fixed with the typical bond lengths of C–O (1.15 Å), C–Pt (1.85 Å), and O–Pt (2.02 Å).

The instability of structure A can be readily understood as follows. The distance between the chemisorbed oxygen atom and the carbon atom in CO is about 1.72 Å if the bond lengths of O–Pt and C–Pt are assumed to be 2.02 Å (the bond length in Pt(111)-p(2×2)-O) and 1.85 Å (the bond length in Pt(111)-p(2×2)-CO), respectively. Note that the bond length of C–O in gas-phase CO<sub>2</sub> is 1.16 Å and will be 1.74 Å if it is stretched by 50%, which is a typical bond stretch at around the transition state for a reaction. Therefore, the distance between the chemisorbed oxygen and the carbon atom in CO in structure A is close to the distance that is expected to be about the transition state of CO oxidation. It is known that the transition state is a maximum in energy along the reaction coordinate in a reaction. In other words, the distance between the chemisorbed oxygen atom and the carbon atom in CO is too short to be stable in structure A. Very recently, a CO oxidation mechanism has been identified on metal surfaces,<sup>48</sup> and indeed when the distance between the chemisorbed oxygen atom and the carbon atom is

**Table 2.** Comparisons between C–O, C–Metal, and O–Metal (chemisorbed O and metal) Bond Lengths in Coadsorption Systems and That in Pure CO and Pure O Chemisorption Systems

	C–O bond length (Å)	C–M (Pt,Rh,Ru) bond length (Å)	O–M (Pt,Rh,Ru) bond length (Å)
Pt(111)-p(2×2)-(CO+O)	1.14	1.85	2.02
Pt(111)-p(2×2)-CO	1.14	1.85	
Pt(111)-p(2×2)-O			2.02
Rh(111)-p(2×2)-(CO+O) <sup>37</sup>	1.19	1.83	2.06
Rh(111)-( $\sqrt{3}\times\sqrt{3}$ )-CO <sup>40</sup>	1.20	1.83	
Rh(111)-p(2×2)-O <sup>37</sup>			2.00
Ru(001)-p(2×2)-(CO+O) <sup>36</sup>	1.16	1.93	2.06–2.09
Ru(001)-( $\sqrt{3}\times\sqrt{3}$ )-CO <sup>38</sup>	1.17	1.98	
Ru(001)-p(2×2)-O <sup>39</sup>			2.03

1.72 Å the energy is very high compared to the initial state, which is in fact structure B.

It should be pointed out that structure B agrees very well with the experimental results of Schwegmann et al.<sup>43</sup> for Rh(111)-p(2×2)-(CO+O) and is also similar to the Ru(001)-p(2×2)-(CO+O) system of Narloch et al.<sup>42</sup> Some structural parameters of optimized structure B are listed in Table 2. A striking feature in Pt(111)-p(2×2)-(CO+O) can be seen: the bond lengths of C–O and C–Pt in the system are the same as that in Pt(111)-p(2×2)-CO and the distance between chemisorbed oxygen and its nearest Pt neighbors in the coadsorbate system is also identical with that in Pt(111)-p(2×2)-O. To show a comparison with experimental data, the structural parameters of Rh(111)-p(2×2)-(CO+O),<sup>37</sup> Rh(111)-( $\sqrt{3}\times\sqrt{3}$ )-R30°-CO,<sup>46</sup> Rh(111)-p(2×2)-O,<sup>43</sup> Ru(001)-p(2×2)-(CO+O),<sup>42</sup> Ru(001)-( $\sqrt{3}\times\sqrt{3}$ )-R30°-CO,<sup>44</sup> and Ru(100)-p(2×2)-O<sup>45</sup> are also listed in Table 2. In particular, the structure of Rh(111)-p(2×2)-(CO+O) is directly relevant to Pt(111)-p(2×2)-(CO+O) because both Pt and Rh are fcc metals and exhibit a similar reactivity for CO oxidation. It can be seen from these three systems that the local structure, namely the bond lengths of C–O, C–Pt (Rh, Ru), and the distance between chemisorbed oxygen and Pt (Rh, Ru) in coadsorbate systems are very similar to that in CO/Pt (Rh, Ru) and O/Pt (Rh, Ru), respectively. This indicates that the direct interaction between CO and chemisorbed oxygen is very small in these systems and that the bonding is local.

To examine the local bonding further, we calculated the local densities of states for the coadsorbate system as we did for Pt(111)-p(2×2)-CO and Pt(111)-p(2×2)-O shown in the last two sections. A comparison of the local densities of states cutting around CO from Pt(111)-p(2×2)-(CO+O) and Pt(111)-p(2×2)-CO is displayed in Figure 11. They are not absolutely identical: the major difference is that the height of the fourth peak (the mixing states between CO 1π orbitals and metal d states) in Pt(111)-p(2×2)-(CO+O) is slightly lower and the peak width is slightly wider than that in Pt(111)-p(2×2)-CO. Nevertheless, the similarity between these two curves is obvious. Panels a and b in Figure 12 display the plots of local densities of states cutting around oxygen with a radius of 0.4 Å from Pt(111)-p(2×2)-(CO+O) and Pt(111)-p(2×2)-O, respectively. Except for some small differences, which are mainly the height and width of the second peak (the mixing states between the oxygen p orbital and metal d states), these two curves are very similar. These results further support the suggestion that the bonding is local in this system.

This suggestion can be finally confirmed by comparing binding strengths in Pt(111)-p(2×2)-(CO+O) with Pt(111)-p(2×2)-CO and Pt(111)-p(2×2)-O. We estimated the binding

(46) Gierer, M.; Barbieri, A.; Van Hove, M. A.; Somorjai, G. A. *Surf. Sci.* **1997**, *391*, 176.

(47) Xu, Z.; Surnev, L.; Uram, K. J.; Yates, J. T., Jr. *Surf. Sci.* **1993**, *292*, 235.

(48) Alavi, A.; Hu, P.; Deutsch, T.; Silvestrelli, P. L.; Hutter, J. *Phys. Rev. Lett.* **1998**, *80*, 3650.



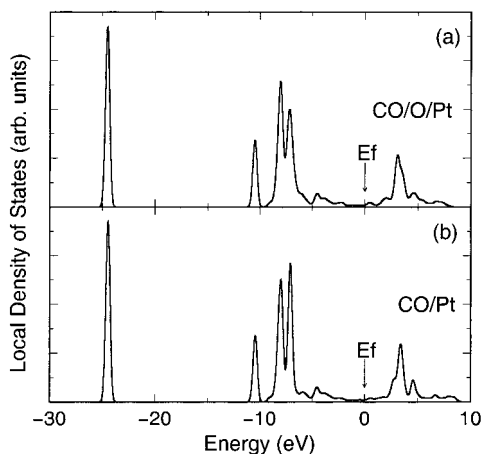


**Figure 11.** Panels a and b are local densities of states cutting a cylinder around CO with a radius of 0.4 Å from Pt(111)-p(2×2)-(CO+O) and Pt(111)-p(2×2)-CO, respectively. The energy scales are shifted so that the Fermi levels are at zero.

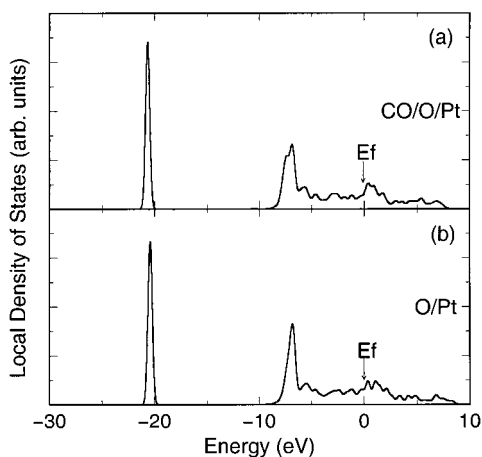


**Figure 12.** Panels a and b are local densities of states cutting a sphere around the chemisorbed O atom with a radius of 0.4 Å from Pt(111)-p(2×2)-(CO+O) and Pt(111)-p(2×2)-O, respectively. The energy scales are shifted so that the Fermi levels are at zero.

strength between CO and Pt,  $\Delta E_{\text{CO,O/Pt}}$ , in Pt(111)-p(2×2)-(CO+O) in the following equation

$$\Delta E_{\text{CO,O/Pt}} = E_{\text{CO/O/Pt}}^{\text{total}} - E_{\text{O/Pt}}^{\text{total}} - E_{\text{CO}}^{\text{total}}$$

where  $E_{\text{CO/O/Pt}}^{\text{total}}$ ,  $E_{\text{O/Pt}}^{\text{total}}$  and  $E_{\text{CO}}^{\text{total}}$  are the total energies of Pt(111)-p(2×2)-(CO+O), Pt(111)-p(2×2)-O, and a CO molecule, respectively. Effectively,  $\Delta E_{\text{CO,O/Pt}}$  is the chemisorption energy of CO on oxygen-precovered Pt(111). The binding strength between O and Pt in Pt(111)-p(2×2)-(CO+O),  $\Delta E_{\text{O,CO/Pt}}$ , is approximated as

$$\Delta E_{\text{O,CO/Pt}} = E_{\text{CO/O/Pt}}^{\text{total}} - E_{\text{CO/Pt}}^{\text{total}} - E_{\text{O}}^{\text{total}}$$

where  $E_{\text{CO/Pt}}^{\text{total}}$  and  $E_{\text{O}}^{\text{total}}$  are the total energies of Pt(111)-p(2×2)-CO and an oxygen atom, respectively.  $\Delta E_{\text{O,CO/Pt}}$  is, in fact, the oxygen atom chemisorption energy on CO-precovered Pt(111). The binding strengths are listed in Table 4. It can be seen that the binding strength between the oxygen atom and Pt in the coadsorbate system is almost identical with that in the pure oxygen atom chemisorption system, which means the presence of chemisorbed CO having little effect on oxygen atom chemisorption in Pt(111)-p(2×2)-(CO+O). It is also clear that the presence of the oxygen atom does not significantly influence

**Table 3.** Comparisons between Chemisorption Energies of CO and O Pt(111)-p(2×2)-(CO+O) and That in Pt(111)-p(2×2)-CO and Pt(111)-p(2×2)-O

	chemisorption energy (eV)	
	CO	O
Pt(111)-p(2×2)-(CO+O)	1.51	4.39
Pt(111)-p(2×2)-CO	1.55	
Pt(111)-p(2×2)-O		4.43

the binding of CO with Pt, because the binding strength between CO and Pt in the coadsorbate system is very similar to that in the pure CO chemisorption system. We can conclude that bonding is very local in this system.

It should be noted that the distance between the carbon atom in CO and the chemisorbed oxygen atom is quite short, being about 3.2 Å. Then the question is: why does the chemisorbed oxygen atom have little effect on CO chemisorption nearby despite the fact that oxygen has a very high electronegativity? Because of the high electronegativity of oxygen, one would expect that a chemisorbed oxygen atom should withdraw some electrons, and therefore significantly weaken the C–Pt bond. In fact, this argument is widely used in the literature. This puzzle can be explained as follows. In Pt(111)-p(2×2)-(CO+O), shown in Figure 10b, the oxygen atom bonds with three Pt atoms while the CO bonds with a single Pt atom. There is no direct competition for bonding over the same metal atom from the adsorbates. Figure 13a shows a 2-D contour plot of the total valence charge densities in a cut through the CO and the chemisorbed oxygen atom from Pt(111)-p(2×2)-(CO+O). The same cuts from Pt(111)-p(2×2)-CO, Pt(111)-p(2×2)-O, and Pt(111) are displayed in Figure 13, panels b, c, and d, respectively. To show a comparison, the same scale is used in these plots. The following features can be observed in the figure. First, there is a small decrease of electron density along the bond axis in the metal atom that is bonded with a CO molecule or an oxygen atom, while a small increase in electron density in the metal atoms along the orthogonal direction of metal–CO or metal–O bonds exists. The latter can be seen clearly in the charge density difference between Pt(111)-p(2×2)-(CO+O) and Pt(111), shown in Figure 14. Second, there is a considerable charge density distortion near the bonding region in the metal atom to which the CO molecule or oxygen atom bonds. For example, some charge densities of the top sphere of Pt 1 in Figure 13, panels a and b, move to the bonding region between the CO molecule and the Pt atom. Third, the chemisorbed oxygen atom or the CO molecule does not significantly affect the charge distribution of the next nearest neighbors.

These features are quantitatively supported by the results in Table 4, in which the total valence electrons in certain spheres around some Pt atoms and C and O atoms are listed. A radius of 1.0 Å, which is about the distance from a metal atom center to the charge density minimum along the metal–C or metal–O bond axis, is used for some Pt atoms to avoid cutting into a carbon or oxygen atom. A radius of 1.0 Å was chosen for the chemisorbed oxygen atom for the same reason. A radius of 1.39 Å, which is the radius of a Pt atom in bulk Pt, is also used for a Pt atom in the second layer. It can be seen that the chemisorbed oxygen is indeed negatively charged, compared to the oxygen atom in the gas phase. However, there is no significant change in charges around the carbon and oxygen atoms in CO from Pt(111)-p(2×2)-(CO+O) and Pt(111)-p(2×2)-CO in comparison with gas-phase CO. Perhaps the most interesting result in Table 4 is that there is no significant change of electrons in the spheres of Pt atoms with a 1.0 Å radius. In particular, no substantial

**Table 4.** Total Valence Electrons in Spheres Cutting around Some Pt, O<sub>a</sub>, O, and C Atoms in Pt(111)-p(2×2)-(CO+O<sub>a</sub>), Pt(111)-p(2×2)-CO, Pt(111)-p(2×2)-O<sub>a</sub>, Pt(111), CO Molecule, and an Isolated Oxygen Atom, Where O<sub>a</sub> Is the Chemisorbed O Atom, O Is the O Atom above the C Atom<sup>a</sup>

	Pt1, $r = 1.0 \text{ \AA}$	Pt2, $r = 1.0 \text{ \AA}$	Pt3, $r = 1.00, 1.39 \text{ \AA}$	O <sub>a</sub> , $r = 1.0 \text{ \AA}$	O, $r = 0.7 \text{ \AA}$	C $r = 0.4 \text{ \AA}$
Pt(111)-p(2×2)-(CO+O <sub>a</sub> )	6.07	6.07	6.05, 8.99	5.76	4.18	0.41
Pt(111)-p(2×2)-CO	6.05	6.08	6.06, 8.97		4.18	0.41
Pt(111)-p(2×2)-O <sub>a</sub>	6.09	6.05	6.05, 8.99	5.74		
Pt(111)	6.06	6.06	6.06, 8.97			
CO					4.18	0.41
O				5.06		

<sup>a</sup> The radius of  $1.0 \text{ \AA}$  was chosen for Pt atoms because it is approximately the distance between a Pt atom center and the minimum of valence electron densities along the Pt–O<sub>a</sub> or Pt–C bond axes. The radius of  $1.0 \text{ \AA}$  was used for O<sub>a</sub> for the same reason. The radius of bulk Pt is  $1.39 \text{ \AA}$ . The choice of radii of  $0.7 \text{ \AA}$  for O and  $0.4 \text{ \AA}$  for C is somewhat arbitrary. However, the same trend can be observed with different radii.

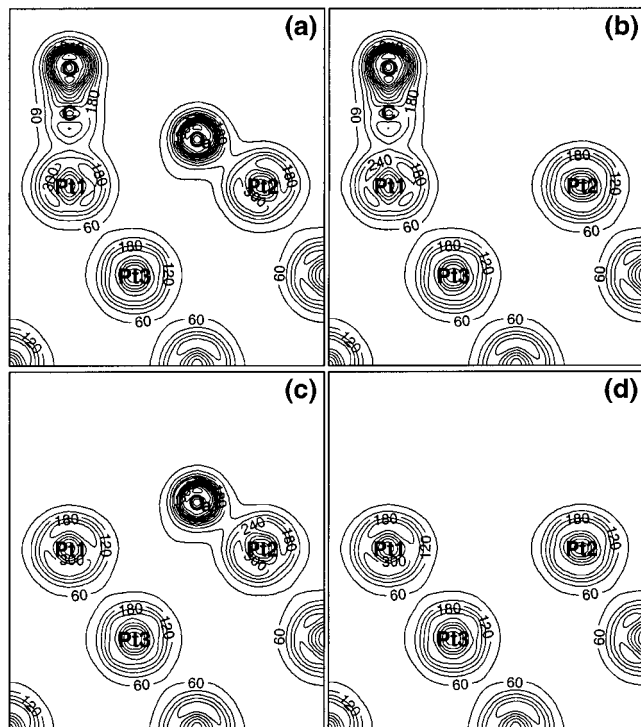


**Figure 13.** 2D contours of total valence charge densities from Pt(111)-p(2×2)-(CO+O) (a), Pt(111)-p(2×2)-CO (b), Pt(111)-p(2×2)-O (c), and Pt(111) (d) respectively, cutting through CO and the chemisorbed O atom in Pt(111)-p(2×2)-(CO+O). The same cut is used for panels b–d. A linear scale is used in unit of  $10^{-3}$  electrons/bohr<sup>3</sup>.

change of charge can be seen in Pt 3, which is the next nearest neighbor of CO or the chemisorbed oxygen. Note that the choice of radii  $0.4$  and  $0.7 \text{ \AA}$  for the C and the oxygen atom above the carbon is somewhat arbitrary, but the same trend can be seen if other radii are used. It is obvious that the presence of CO in Pt(111)-p(2×2)-(CO+O) does not significantly affect the charge density distribution around the chemisorbed oxygen atom and vice versa.

By examining all the calculated quantum states in Pt(111)-p(2×2)-(CO+O), we found that the direct bonding between CO and the chemisorbed oxygen atom is negligible. We expect that the bonding of CO and oxygen with Pt atoms will change dramatically if these two species share bonding with the same Pt atoms. An example is shown in Figure 15, in which the chemisorbed oxygen atom is on the hollow site and CO adsorbs on the bridge site. Alavi et al.<sup>48</sup> reported in a recent study that the structure in Figure 15 is about  $0.5 \text{ eV}$  higher in energy than structure B, shown in Figure 10b. Density Functional Theory calculations show that the CO chemisorption energy on the bridge site of Pt(111) is very similar to that for CO on the top

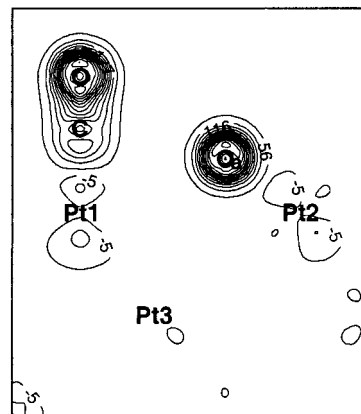


**Figure 14.** The total valence charge density difference between Pt(111)-p(2×2)-(CO+O) and Pt(111). The same cut is used in Figure 13.

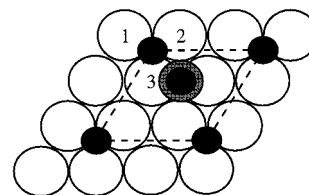


**Figure 15.** Schematic illustration of the bonding competition between CO and chemisorbed O with Pt 3.

site and there is no significant direct repulsion between CO and the chemisorbed oxygen. Therefore, we believe that the energy increase of  $0.5 \text{ eV}$  in the structure shown in Figure 15 compared to structure B in Figure 10b is mainly due to the bonding competition of CO and the oxygen atom with Pt atom 3. The fact that structure A, shown in Figure 10a, is less stable than structure B can also be understood by using the simple picture discussed above: there is a competition for bonding between the CO and the oxygen with a Pt atom in structure A, leading to an increase in energy. In a recent study, Ge et al.<sup>39</sup> reported a very strong site symmetry dependence of repulsive interactions between chemisorbed oxygen atoms on Pt(100)-(1×1). Namely, binding energies are almost identical on bridge sites when the oxygen coverage is increased from  $0.25$  to  $0.5 \text{ ML}$ , while there is a sharp drop in binding energy for oxygen on hollow sites with the same oxygen coverage change. This can be explained in a similar way: for oxygen on the bridge sites, each oxygen atom bonds directly with two Pt atoms and the local bonding does not change significantly from an oxygen coverage of  $0.25$  to  $0.5 \text{ ML}$ . Therefore, the binding energies are very similar. On the other hand, when oxygen atoms adsorb on the hollow sites, each oxygen bonds with four Pt atoms and the local bonding changes considerably from an oxygen coverage of  $0.25$



to 0.5 ML: At 0.25 ML, there is no strong bonding competition between oxygen atoms with metal atoms. However, at 0.5 ML, each oxygen atom has to share bonding to metal atoms with other O atoms. Consequently, the binding energy at 0.5 ML is lower than that at 0.25 ML. A similar explanation was given by Ge et al.<sup>39</sup>

It should be emphasized that the conclusion that bonding is very local and the interaction between adsorbates is short range in nature is only valid to a certain degree. There is evidence that oxygen chemisorption affects CO chemisorption or vice versa in Pt(111)-p(2×2)-(CO+O): very weak direct bonding between the oxygen and CO does exist; the local densities of states, say cutting around CO, in Pt(111)-p(2×2)-(CO+O) are not absolutely identical with that from Pt(111)-p(2×2)-CO; and the binding strength between CO and Pt in Pt(111)-p(2×2)-(CO+O) is slightly weaker than that in Pt(111)-p(2×2)-CO. One might well use these results to support the long-range interaction argument. Nevertheless, it is clear that the main chemical properties of these systems, such as bond lengths and bond strengths, are essentially short range in nature. This conclusion is also confirmed in larger unit cell (8 Pt atoms/layer) calculations. We believe that this simple local bonding picture presented in this section should be useful in surface science and catalysis in understanding geometrical structures of chemisorption systems and surface reaction mechanisms. In fact, it can be used to explain many features of the CO oxidation chemistry on Pt(111).<sup>48,49</sup>

#### 4. Conclusions

The work reported here represents one of the first attempts to understand the interactions between adsorbates using Density Functional Theory. We have performed ab initio total energy calculations for Pt(111), Pt(111)-p(2 × 2)-CO, Pt(111)-p(2×2)-

O, and Pt(111)-p(2×2)-(CO+O). All important structural parameters were obtained by optimization. For the clean Pt(111), it was found that there is no surface relaxation. In Pt(111)-p(2×2)-CO and Pt(111)-p(2×2)-O, the bond lengths of C–O, Pt–C, and Pt–O (the chemisorbed oxygen) are 1.14, 1.85, and 2.02 Å, respectively, which agree with experimental values very well. The bonding between CO and Pt(111) has been quantitatively analyzed. The bonding between oxygen atoms and Pt(111) has been studied in detail and an interaction framework has been proposed. Perhaps most importantly, the interaction between CO and O in Pt(111)p(2×2)-(CO+O) has been studied in detail. Interestingly, the local structures, such as the bond lengths of C–O, Pt–C, and Pt–O (the chemisorbed oxygen) in Pt(111)-p(2×2)-(CO+O) are the same as Pt(111)-p(2×2)-CO and Pt(111)-p(2×2)-O, respectively. The total valence charge density distributions around Pt–C–O and O–Pt in the coadsorbate system are also very similar to that in Pt(111)p(2×2)-CO and Pt(111)p(2×2)-O, respectively. There are clear similarities in the local densities of states cutting around CO between Pt(111)-p(2×2)-(CO+O) and Pt(111)-p(2×2)-CO. Similarities of the local densities of states cutting around chemisorbed oxygen between the coadsorbate system and Pt(111)-(2×2)-O also exist. It has been found that the binding strength between CO and Pt in Pt(111)-p(2×2)-(CO+O) is very similar to that in Pt(111)-p(2×2)-CO. The binding strength between the chemisorbed oxygen and Pt in Pt(111)-p(2×2)-(CO+O) is also almost identical with that in Pt(111)-p(2×2)-O. Therefore, it is concluded that the bonding is local and the interaction between adsorbates is mainly short range in nature. We believe that these results are very useful in understanding surface chemistry and catalysis.

**Acknowledgment.** This work has been supported by the EPSRC.

JA983363W

(49) Ray, N. K.; Anderson, A. B. *Surf. Sci.* **1982**, *119*, 35.